

## SHORT COLUMN SEDIMENTATION EQUILIBRIUM ANALYSIS FOR RAPID CHARACTERIZATION OF MACROMOLECULES IN SOLUTION

Thomas M. Laue University of New Hampshire Department of Biochemistry Durham, NH 03824

### Introduction

Short column sedimentation equilibrium analysis offers many advantages for researchers wanting quick, sure characterization of the solution properties of macromolecules. Presented here is a list of when short column methods are an appropriate choice, a brief theoretical treatment and an overview of short column sedimentation methods, including ones diagnostic for self-association and nonideality. Short column methods were first described by Van Holde and Baldwin in 1958 (1), and centerpieces specifically designed for these methods were described by Yphantis in 1960 (2). Their distinguishing characteristics are (Fig. 1):

1. The parallel rows of four, small, sample viewing (1.2 mm diameter) holes 4 mm apart.
2. The two rows of larger (2.4 mm) holes used for filling the cell.
3. The connecting groove between the fill hole and sample viewing holes.

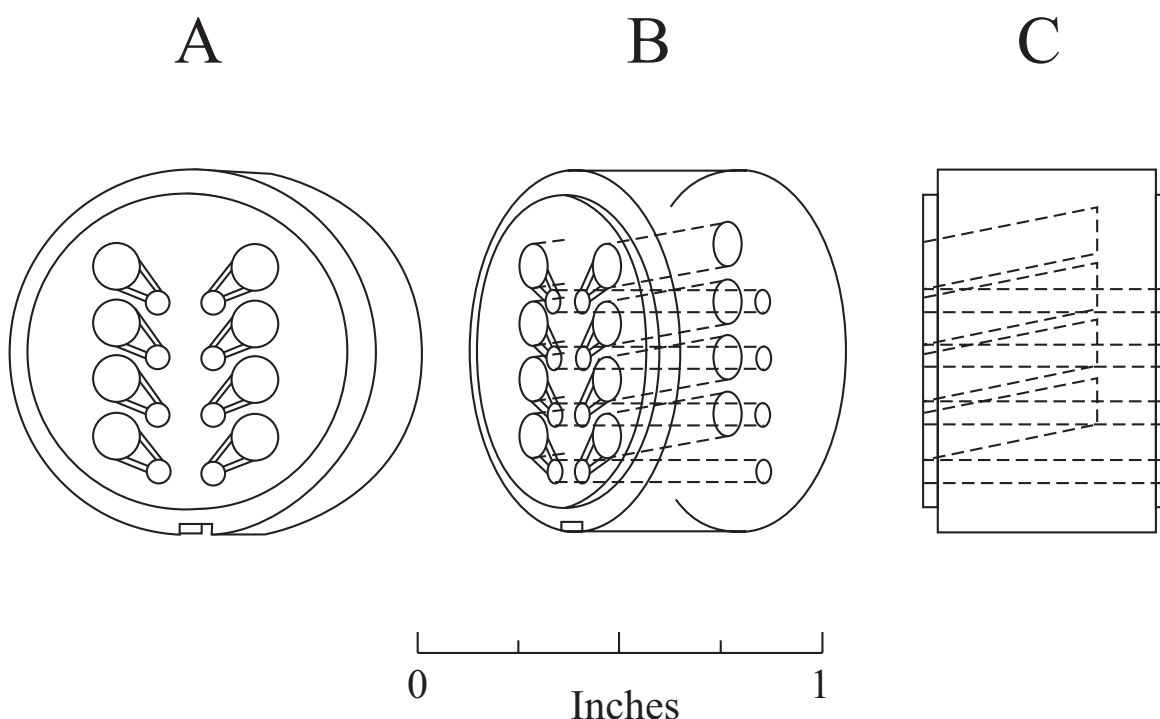


**Figure 1.** Eight-channel, short column centerpiece that allows the viewing of four solution-solvent pairs. Direction of the gravitational field is toward the keyway. The small holes are observation channels, and the large holes are filling reservoirs. The holes on the left half hold the solvent only, and those on the right half, the solvent with macromolecule. On acceleration the contents of a filling reservoir drain through the groove into the corresponding observation channel. The holes for the filling reservoirs are tapered so that they empty completely. For filling, the centerpiece is positioned in the cell housing as shown in view A, with the top-most holes referred to as channel A and the bottommost as channel D.

Despite their early development, short column sedimentation equilibrium methods did not enjoy extensive use with the early users of sedimentation equilibrium for several reasons:

1. Manual data acquisition from short columns required nearly the same amount of time as from longer columns and did not yield as much information per data set
2. They required higher concentrations of material
3. They could not be used with the photoelectric scanner of the Model E
4. They often required that a separate experiment be conducted to measure the sample concentration. However, a great deal has changed in the intervening years, and all of these limitations have been overcome.

Data acquisition takes seconds now, whereas it could require days in the early '60s. Thus, there is a distinct advantage to the rapid equilibration available with short columns in that they provide at least a 20-fold increase in the number of samples that can be examined in a given period of time. Thus, with a few exceptions, the quantity of information available from short columns exceeds that from the longer columns. Short column centerpieces can be used with the photoelectric scanner of the Proteomelab XL-A analytical ultracentrifuge, hence lower concentrations may be used and a separate concentration determination is not necessary. Finally, improvements in data analysis (3, 4) have made it possible to combine the data from several short column experiments in order to evaluate the molecular parameters of interest. These same programs eliminate the need for separate concentration determinations for interference optics, saving material and time. With these advances, the advantages of short columns make them the method of first-choice for many routine analyses.

The advantages of short column centerpieces are:

1. Only a small volume (15  $\mu\text{L}$  vs. 100  $\mu\text{L}$ ) of material is required at moderate concentrations (0.1 OD)
2. Short equilibration times are needed (60–90 min vs. 16–18 h for most molecules)
3. A large number of samples can be examined simultaneously
4. There is minimal radial redistribution of solutes

The first advantage is a clear benefit when only small quantities of a material are available for analysis. Even more attractive is the possibility of recovering much of the sample volume (75–90%) after analysis. When it is desirable to examine a sample over a wide range of buffer conditions, the first three advantages are of interest. The final advantage is of particular interest when it is necessary to perform titrations or when characterizing an association between dissimilar macromolecules (*i.e.*, heteroassociation).

These advantages are so compelling, it is useful to outline when it is better to use the longer, 3-mm column centerpieces. The longer columns are better to use when:

1. Examining heterogeneous samples
2. Examining low molecular weight materials
3. When only very dilute samples are available
4. When the sticking of a sample to centerpiece walls makes it desirable to exploit the lower surface area-to-volume ratio of the 3-mm column centerpieces

Below are described some typical applications for short column centerpieces. These uses have been arranged in sequence ranging from the most simple to the more complicated. It is important to note, however, that the basic methodology is the same and that it is the data analysis and interpretation that vary in complexity. This has the fortunate consequence that even if diagnostic analysis indicates that a chemical system is exhibiting complicated behavior, it is often only the method of analysis that needs to be modified, and there is no need to repeat experiments.

## Methods

### Sample Preparation

There are no special sample preparations necessary for short column sedimentation equilibrium. Samples used for absorbance detection should have an optical density between 0.1 and 1.5 at the wavelength of interest. Samples

for Rayleigh interference detection, as used in the Model E, should have greater than 0.2 fringe (60 µg/mL) initial concentration. For both optical systems, it is preferable that the sample be at dialysis equilibrium with the solvent. This can be achieved either by exhaustive dialysis (1000:1 volume:volume dialysate to sample, with stirring for 72 h against three changes of buffer) or, more rapidly (10 min) and conveniently using centrifugal gel filtration (5). Our experience is that this method is every bit as thorough as exhaustive dialysis, and, except in cases where sample is lost by binding to the gel matrix or when slow kinetics prohibit its use (e.g., refolding of a protein from a denaturant), it is the preferred method.

### **Cell Handling**

Select a centerpiece made from a material that does not interact with the macromolecules of interest. Short column centerpieces are made of Kel-F, which is the least likely to absorb H<sub>2</sub>O or to bind materials from the solution. However, Kel-F should not be used routinely above 40,000 rpm, since deformation of the centerpiece is likely.

Because of the high surface-area-to-volume ratio, the centerpiece must be scrupulously clean to prevent sample contamination. When cleaning, be careful not to scratch the surfaces of the centerpiece. The surface and holes should be scrubbed with a nonabrasive detergent (SDS works well) using nonabrasive scrubbers. We have found that nonwoven cellulose and polyester cleanroom wipes (e.g., DURX 770, Berkshire Corp., Great Barrington, MA) are useful for wiping the faces of the centerpieces, while microswabs (e.g., TX732, Berkshire Corp., Great Barrington, MA) are useful for cleaning the holes. Thoroughly rinse the centerpiece with distilled, deionized water. For this latter step, it is useful to equip a small hose with a micropipette tip to direct a concentrated stream into the holes. Dry the centerpiece with a gentle stream of dry nitrogen gas, again using a micropipette tip to blow out the holes. It is possible to include special cleaning steps (e.g., rinsing with EDTA, soaking in protease inhibitors, use of organic solvents) as long as there is no chemical reaction with the centerpiece materials and as long as the reagents can be removed without leaving any residue. Centerpieces should be cleaned and dried immediately after use and should be stored wrapped in nonshedding paper.

Cell assembly is as described in the manual for the Proteomelab XL-A, except that the top window is not put into the cell housing until after the centerpiece is filled. For absorbance detection, the top window should be in a narrow aperture holder (e.g., an old Rayleigh-mask window holder), since this holder masks the incident beam, providing a uniform light pulse over the radial extent of the column. However, adequate results for most purposes are obtained using the wide-aperture window holders ordinarily used for absorbance detection. Either window holder may be used with the Rayleigh system.

Serial dilutions are made using the dialysate. In order to eliminate any dust, samples should be spun in Eppendorf tubes in a microfuge for 5 min. Alternatively, the samples may be filtered. Failure to do this step usually has no adverse effects unless large aggregates are present and very low speed analyses (e.g., <3000 rpm) are performed.

### **Cell Assembly and Filling**

A complete bottom window and a clean centerpiece are inserted into the cell housing and pressed down using a lint free tissue until the window is at the bottom of the housing. A jet of dry nitrogen gas can be used to blow away any dust on the window prior to inserting the centerpiece and, again, just before filling. The cell housing is positioned with the keyway towards you so that the filling grooves form a "V" (Fig. 1A). The larger holes are filled, with the holes on the left for solvent and those on the right for solution. Solvent-solution pairs are designated A-D, going from those closest to the center of rotation (A, the furthest from you during filling) to those closest to the edge of the rotor (D, the closest to you during filling). Filling is accomplished with a 20-µL variable pipetter equipped with a microcapillary tip. The solvent holes are filled with 20 µL of solvent. The solution holes are first filled with 5 µL of FC-43\* fluorocarbon (used as a base fluid, below) and 14 µL of sample, with the most concentrated sample going in position A and the most dilute in D. Cell assembly is then completed in the normal manner, except that no filling-hole screws are necessary. Rapidity of filling and assembly is essential to minimize the effects of evaporation.

Any inert, dense liquid can be used as a base fluid. FC-43 provides a clear, "square" bottom, and, because its refractive index is close to that of water, does not produce as much reflection at the interface as do other base fluids. FC-43 itself is extraordinarily inert, though contamination with hydrocarbons can lead to interactions with solution components. Should this be the case (evidenced by a buildup of a layer of material at the interface) the FC-43 can be extracted with concentrated H<sub>2</sub>SO<sub>4</sub> followed by exhaustive rinsing with distilled, deionized water.

## Short Column Operation

The rotor is loaded and the cells aligned as described in the Proteomelab XL-A manual. The samples will transfer to the viewing holes at about 5000 rpm. Rotor speeds are chosen as for a longer column equilibrium run such that the expected value of  $\sigma$  is in the range between 2 and 10:

$$\sigma = \frac{M(1 - \bar{v}\rho)\omega^2}{RT} \quad \text{where } \omega = \frac{\text{RPM } \pi}{30} \quad (1)$$

and  $\bar{v}$  is the partial specific volume of the solute,  $\rho$  is the solution density,  $R = 8.3144 \times 10^7$  and  $T$  is the temperature in K. Note that a rough estimate is all that is required, so that for  $\sigma = 3$  an initial choice of speed can be estimated from:

$$\text{RPM} = \sqrt{\frac{150RT}{\pi M(1 - \bar{v}\rho)}} \approx 2 \times 10^6 \sqrt{\frac{1}{M}} \quad (2)$$

where the approximation is valid for aqueous buffer  $\rho \approx 1$ , at temperatures near 25°C and for materials having  $\bar{v}$  near 0.7 mL/g. If  $M(1 - \bar{v}\rho)$  is completely unknown, it will be necessary to observe the redistribution of the solute at several rotor speeds, starting at about 2500 rpm. However, to ensure complete transfer of the sample, the rotor should be brought to 8000 rpm for a couple of minutes before dropping the rotor speed back to 2500 rpm.

When 14  $\mu\text{L}$  of solution are used, the column height (from meniscus to FC-43 interface) should be 700-800  $\mu\text{m}$ . A scan should be made of the cell immediately after reaching speed to ensure sample transfer and to test for leaks. It should be noted that at very low rotor speeds (<4000 rpm), both the meniscus and base are distorted by the earth's gravitational field, leading to boundaries with a very broad appearance. In our experience, solution transfer is not a problem, and leaking, which is also rare, occurs only at high speeds and between holes along the radial axis.

## Estimating the Equilibration Time

One of the greatest advantages of short columns is the rapid achievement of equilibrium, which, since the time to equilibrium is proportional to the square of the column height, is about 16 times faster than for 3-mm columns. The length of time to reach equilibrium can be estimated from the formulas given by van Holde and Baldwin (1) or can be determined empirically by making successive overlay scans 10 min apart, looking for any further movement of the concentration gradient. (A systematic "tail" at the base or meniscus is a good diagnostic for nonequilibrium.) For most 10–200-kDa proteins, we typically begin testing for equilibrium after 45 min at speed. Very large molecules will take longer (e.g., *E. coli* ribosomes,  $M_w = 1.46 \times 10^6$  require 250–300 min (4)), and viscous solvents will slow down equilibrium by an amount directly proportional to the viscosity. On the other hand, small molecules and nonideal solutes tend to reach equilibrium faster than might be expected.

## Data Acquisition

Precise, closely spaced data are required for good analysis. Consequently, the point density should be as high as possible. This means that for the Proteomelab XL-A absorbance system, a step scan should be used with 0.001-cm step size and with four repetitions per step. To save time, only those portions of the cell where light is visible should be scanned. Radial resolution is not a problem with the Rayleigh optics. The starting and ending radii for channels A through D can be obtained from the initial scan and, once determined, recorded for use in future experiments. Between 50 and 100 data points should be acquired for each channel.

For absorbance detection, the 4-mm center-to-center spacing of the cell holes requires that the flash lamp timing be set slightly differently from that ordinarily used. Optimum results are obtained if a value between 1.65° and 1.75° is used as the spacing between the holes (ordinarily set for 2.5°). The best timing can be determined using the method described in the Proteomelab XL-A operating manual.

## Data Editing

Data from the meniscus and base regions may need to be eliminated from analysis due to unavoidable refractive effects at the top and bottom of the cell. If it is desirable to determine average molecular weights with reference to the loading concentration, it is best if data are removed symmetrically about the midpoint of the channel. Otherwise, only remove points that are obviously affected by the discontinuities at the menisci (4).

## Methods for Specific Applications

Aside from rapid surveys and cases where there is limited material, short columns are especially useful for the rapid determination of the association state of an oligomer; for examining the effects of small ligands on macromolecular associations and for the study of heteroassociations (i.e., where mixtures of unlike macromolecules interact). This suitability stems from the fact that component fractionation is constrained by the short radial distance. There are a few additional suggestions for using short columns in these applications.

### Determination of the Stoichiometry of an Oligomer

This is determined simply by measuring the molecular weight of the molecule under native conditions, comparing it to the molecular weight determined under fully denaturing conditions. The molecular weight for the native material is determined at four different loading concentrations, one for each of the channels of a short column centerpiece. Typically, the concentration in channel A is near 1 OD for the absorbance system, or 1 mg/mL for the Rayleigh system, with channels B–D containing a serial 1:2 dilution of the channel A concentration. Only 35  $\mu\text{L}$  of solution are needed to make the dilutions: 14  $\mu\text{L}$  for each channel and 16  $\mu\text{L}$  for the serial dilution (assuming 2–3  $\mu\text{L}$  are lost to the walls). Cell loading is described above. When the solutions are run, the redistribution of the solute will cause the absorbance ranges in the different channels to overlap and to cover an absorbance range from near zero to 2 OD (depending on rotor speed, of course).

The molecular weight of the denatured material can be determined a number of different ways. If the oligomer consists of only one type of monomer, a second cell should be prepared that contains the same sample under fully denaturing conditions. The two denaturants most commonly used for sedimentation analysis of proteins are 8 M urea and 6 M guanidine HCl (6, 7). Of these, guanidine has been better characterized for use in sedimentation and, at 6 M, has minimal effect on  $\bar{v}$ , even for glycoproteins. It is important to realize that guanidine *can and does* influence  $\bar{v}$  (7, 8), but that these effects advantageously cancel at 6 M. Serial dilutions are made with the 6 M guanidine buffer and the second cell loaded as described above. If the oligomer consists of nonidentical chains, the chains should be isolated and analyzed separately under denaturing conditions. The cells should be balanced and loaded into the rotor as described in the manual.

The initial rotor speed should be chosen as described above, using an estimate (if available) of  $M$  for the native material. Should the initial rotor speed prove to be too high (e.g., the protein is highly polymerized and the absorbance gradient is very steep with material compressed at the bottom), it is worthwhile to stop the run and shake the cells to redistribute the contents. Simply lowering the rotor speed will result in an undue wait for re-equilibration. After the data have been acquired at the lowest rotor speed, the speed should be increased until the ratio of the square of the rotor speeds is 1.4 or greater (e.g., if the initial rotor speed was 20,000 rpm, then 24,000 rpm would be a good choice, since  $[24,000/20,000]^2 = 1.44$ ). Finally, it is useful to examine the solution at a rotor speed high enough that the ratio of the square of this speed to the first is 3 or greater (e.g.,  $[36,000/20,000]^2 = 3.24$ ). The use of multiple speeds will provide data that can be used diagnostically (below) and will help ensure that suitable gradients will be developed in all channels under analysis.

### Titration with Small Ligands

Titration can be made either of two ways. The first and preferred method is to dialyze a sample against a range of ligand concentrations. This is done most conveniently using centrifugal gel filtration (5). Dialysis sets the concentration of free ligand equal to the concentration of ligand in the dialysate (or in the column). Since sample and reference have the same free ligand concentration, any optical effects due to the redistribution of the ligand during sedimentation can be neglected. The second titration method is to simply add the ligand directly to the sample. With this method only the total concentration of ligand is known, and systematic errors in the determination of ligand affinities are possible. In cases where only qualitative results are of interest, this method is satisfactory, consumes less material and is much faster. Either method works because small ligands simply do not form significant gradients over the length of a short column. An estimate of the concentration gradient of the ligand due to sedimentation can be made using:

$$\Delta C \approx 2.5 \times 10^{-3} C_0 \sigma \quad (3)$$

where  $C_0$  is the concentration of the ligand and  $\sigma$  is its reduced molecular weight (Eq. 1). It can be seen that even fairly large ligands can be used if  $C_0$  and  $\sigma$  are kept low enough.

## Examination of Heteroassociations

Again, the lack of fractionation of solutes in short columns is an advantage when it is desirable to examine the interactions between unlike macromolecules. Each macromolecule should be equilibrated with the solvent (as described above) and analyses of the individual components must be made so that the behavior of the mixtures can be interpreted properly. It is best to examine heteroassociating systems at a variety of rotor speeds using several different loading concentrations and, if possible, covering a range of mole ratios of components (8, 9). The detailed analysis of these sorts of systems is outside the scope of this review, but specific examples of how these systems can be analyzed are available (8, 9).

## Overview of Data Analysis

There are three levels of analysis of short column sedimentation data. The first level is a qualitative assessment of the macromolecular behavior using diagnostic graphs. At this level the questions are more general, addressing whether or not the system is homogeneous, whether or not nonideality is significant and assessing whether or not a mass action association is occurring. At this level of analysis, a reasonable estimate of the monomer molecular weight is often possible, but quantitative determination of thermodynamic parameters is not. The second level of analysis consists of combining data sets from several short column experiments and fitting the ensemble to models using nonlinear least squares methods (3). Such analyses can provide estimates of thermodynamic parameters like the monomer molecular weight, association constants, association stoichiometries and nonideality coefficients. The confidence interval, *i.e.*, estimates of the precision, for these parameters also can be determined. However, the accuracy of the analysis depends on using the correct model to describe the system. If there is only one plausible model, and it fits the data adequately, then analysis can end at this second level. For many systems, though, a third level of analysis is necessary. This level consists of testing a variety of plausible models and choosing which ones adequately describe the data. Often there is no truly unique model. However, this ambiguity is not due to limitations of short columns nor of sedimentation, but rather intrinsic to the determination of thermodynamic parameters. A detailed discussion of nonlinear curve fitting for sedimentation is outside the scope of this review, but can be found in the literature (3, 4), and some specific applications of nonlinear curve fitting methods to short column data are listed in Refs. 8–10. The remainder of this note will focus on the first level of analysis.

An average molecular weight determination is the simplest and most rapid analysis of short column equilibrium data. The concentration and rotor speed dependence of these determinations form the basis of the diagnostic graphs described below. Using the absorbance system, the molecular weight can be estimated from the slope of the graph of  $\ln(Abs)$  versus  $r^2/2$ . These graphs are available from within the Proteomelab XL-A user interface. Unless heterogeneity or nonideality are particularly severe, graphs of  $\ln(Abs)$  versus  $r^2/2$  should be sensibly linear. The slope of this line is  $\sigma$  (Eq. 1). For the Rayleigh system, which gives only the relative concentration,  $\sigma$  should be determined using a nonlinear least squares approach. When combined with  $\bar{v}$ ,  $\rho$ ,  $\omega^2$ ,  $R$  and  $T$ ,  $\sigma$  yields the molecular weight:

$$M = \frac{\sigma RT}{(1 - \bar{v}\rho)\omega^2} \quad (4)$$

where values for  $\bar{v}$  and  $\rho$  are readily estimated from sample and buffer composition (6). If  $\bar{v}$  is unknown, the buoyant molecular weight,  $M_b$ , can be used for the diagnostic graphs described below:  $M_b = M(1 - \bar{v}\rho) = \sigma/RT\omega^2$ . If the solvent contains a high concentration of one or more components (e.g., 6 M guanidine or 8 M urea), the effects on  $\bar{v}$  of preferential hydration should be taken into account (6, 7).

In addition to graphical analysis, it is also possible to fit the concentration distribution data to functions derived from thermodynamic first principles (2, 3). For a single ideal thermodynamic species, the absorbance profile will be an exponential:

$$Abs = \delta + Abs_0 e^{\sigma\xi} \quad \text{where } \xi = \frac{r^2 - r_0^2}{2} \quad (5)$$

$\delta$  is the baseline offset and  $Abs_0$  is the absorbance at the reference radial position  $r_0$  (2). For a mixture of ideal species, the resultant curve is the sum of exponentials:

$$Abs = \delta + \sum Abs_{0i} e^{\sigma_i\xi} \quad (6)$$

where  $Abs_{0i}$  and  $\sigma_i$  are the reference concentration and reduced molecular weight for the  $i^{\text{th}}$  component, respectively. If a mixture of molecules is present, but the data are treated as though there were only a single sedimenting species, the  $\sigma$  determined is an average value for the components. Under certain conditions, the average value is well-defined and can be used in the analysis of a chemical system (2-4). The weight-average molecular weight is defined as:

$$M_w = \frac{\sum M_i Abs_i}{\sum Abs_i} \approx \frac{\sum M_i C_i}{\sum C_i} \quad (7)$$

where  $M_i$  and  $C_i$  refer to the molecular weight and weight concentration of the  $i^{\text{th}}$  component, respectively. Notice that the scanner provides absorbances and that the average molecular weight requires weight concentrations. It is important to realize that if the weight extinction coefficients differ for the different components, then the molecular weight is not a well-defined average. Under these circumstances, it is preferable to use the Rayleigh optical system.

The same arguments as above regarding the determination of average molecular weights hold true, except that if a nonlinear least squares analysis program is used to fit the data directly and includes  $\delta$ , the *baseline offset*, as a parameter, then it is the z-average that is determined as long as all of the solution column is visible (4, 10):

$$M_z = \frac{\sum M_i^2 Abs_i}{\sum M_i Abs_i} \approx \frac{\sum M_i^2 C_i}{\sum M_i C_i} \quad (8)$$

Notice that the z-average is influenced more strongly by high molecular weight material than is the weight-average.

## Diagnostic Graphs

Two graphs of the molecular weight, one as a function of the total cell loading concentration and the other as a function of the rotor speed, will serve for the initial characterization of a system. Based on these graphs, there are five possible conclusions that can be reached concerning the system:

1. The system is sensibly ideal and homogeneous
2. The system is ideal, homogeneous and exhibits a mass-action association
3. The system is homogeneous and nonideal
4. The system is homogeneous, nonideal and exhibits a mass-action association
5. The system is heterogeneous with regard to mass

The latter category does not exclude possibilities of mass-action association or nonideality. However, while the short column method can be used to detect heterogeneity, it is not especially good at resolving it. Consequently, aside from describing the graphical consequences of heterogeneity, the remainder of this discussion will presume sample homogeneity.

The first diagnostic graph consists of the apparent molecular weight as a function of the midpoint absorbance of each channel (Fig. 2). This graph will be useful for detecting nonideality and mass-action associations. Three conditions may be observed:

1. The molecular weight is constant with changing concentration (absorbance)
2. The molecular weight decreases with increasing concentration
3. The molecular weight increases with increasing concentration

Should the first result be obtained, it suggests that the molecule is behaving ideally. A downward curvature to the molecular weight with increasing concentration indicates thermodynamic nonideality. Useful information may be available from this concentration dependence, and methods for analyzing nonideality are available (11). Increasing molecular weight with increasing concentration is indicative of a mass-action association and will demand a more detailed analysis. Often at high concentrations the reaction is driven to an end point (i.e., the association has an upper limit), in which case the stoichiometry of the largest oligomer may be determined. In other cases the association may be indefinite or experimental complications (e.g., nonideality or limited solubility or availability) may make it difficult to determine an upper limit for the oligomer size. Even in the case of a limited association, the stoichiometry ( $N$ ) becomes difficult to determine as  $1/N$  approaches the precision of the molecular weight estimate (typically 1–3%).

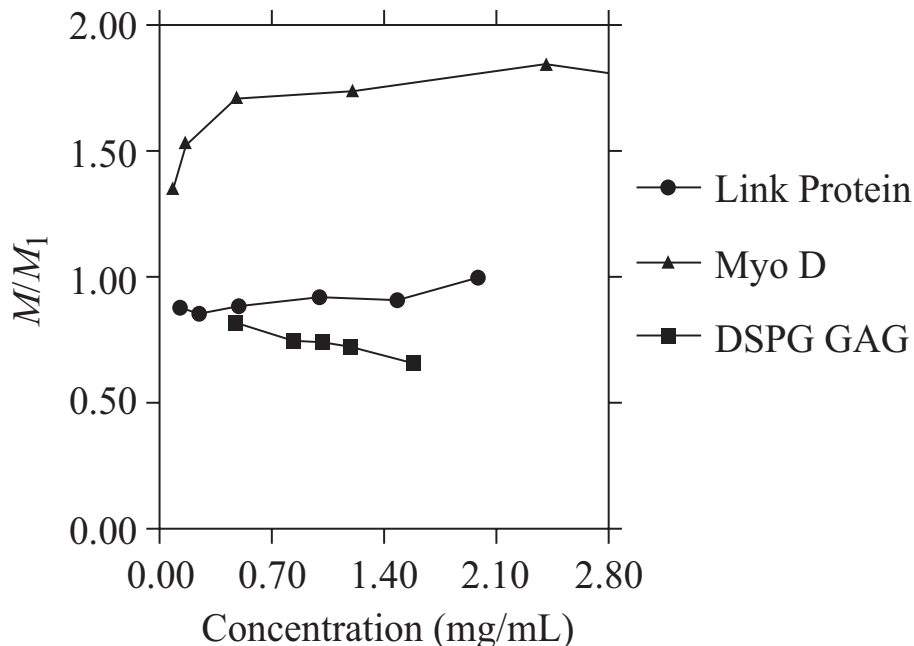


**Figure 2.** Diagnostic graph providing a qualitative characterization of the solution behavior of macromolecules. All data were acquired at a constant temperature between 20 and 25°C. This figure shows the apparent molecular weight as a function of cell loading concentration. Because of the disparity in the monomer molecular weights for the materials shown here, the y-axis is presented as  $M/M_1$ , where  $M_1$  is the "monomer" molecular weight. (●) shows behavior typical for an ideal, nonassociating material. Presented here are the data for bovine articular cartilage link protein ( $M_1 = 260,000$ ) in 0.15 M NaCl, 50 mM Tris (pH 7), 5 mM EDTA. This same sample in 6 M guanidinium buffer gives a monomer molecular weight of 43,000, demonstrating that link protein is a hexamer under nondissociating conditions. (■) shows the behavior typical of a nonideal macromolecule. Presented here are the data for the glycosylaminoglycan chains of bovine articular dermatan sulfate proteoglycan 1 ( $M_1 = 26,000$ ) in the same buffer. These chains are highly charged, leading to the nonideality observed here. The identical monomer molecular weight is obtained when the chains are sedimented in 6 M guanidine containing buffer indicating that they are monomeric in associative buffer. (▲) presents the behavior typical of a mass-action association. The sample in this case is MyoD-bHLH ( $M_1 = 16,000$ ) in 100 mM NaCl, 20 mM acetate, 50 mM Tris, pH 7.6, 2 mM  $\beta$ -mercaptoethanol. These data suggest that MyoD-bHLH undergoes an apparent monomer-dimer equilibrium. However, mass spectroscopy, cDNA sequence analysis and sedimentation in 6 M guanidinium buffer reveal that the true monomer molecular weight is 8000, so the reaction observed here is actually a dimer-tetramer equilibrium.

Graphs of the apparent molecular weight as a function of rotor speed are useful for detecting heterogeneity (Fig.3). They also are important for determining the reversibility of a mass-action association (3). For a homogeneous, noninteracting sample under all conditions, the molecular weight should be independent of rotor speed (3, 4). The same is true for a homogeneous mass-action association, as long as the concentration gradient can be monitored all the way from the meniscus to the base. On the other hand, a systematic decrease in the molecular weight as the rotor speed is increased is diagnostic for sample heterogeneity. Such heterogeneity often is accompanied by a band of material gathering at the FC-43 layer at higher rotor speeds. Because the hydrostatic pressure developed in a short column is quite small, even at high rotor speeds (a few atmospheres), pressure-dependent dissociation is an unlikely cause of decreasing molecular weight with increased rotor speed, thus simplifying the interpretation. Should heterogeneity be suspected, further fractionation of the sample (e.g., by size-exclusion chromatography) is required. For a heterogeneous mass-action association, the apparent molecular weight can exhibit rotor-speed dependence depending on how tight the oligomerization is and whether all reactants are present in the stoichiometrically correct amounts. Under these circumstances, these graphs are not useful and more detailed analysis will be required (see above).



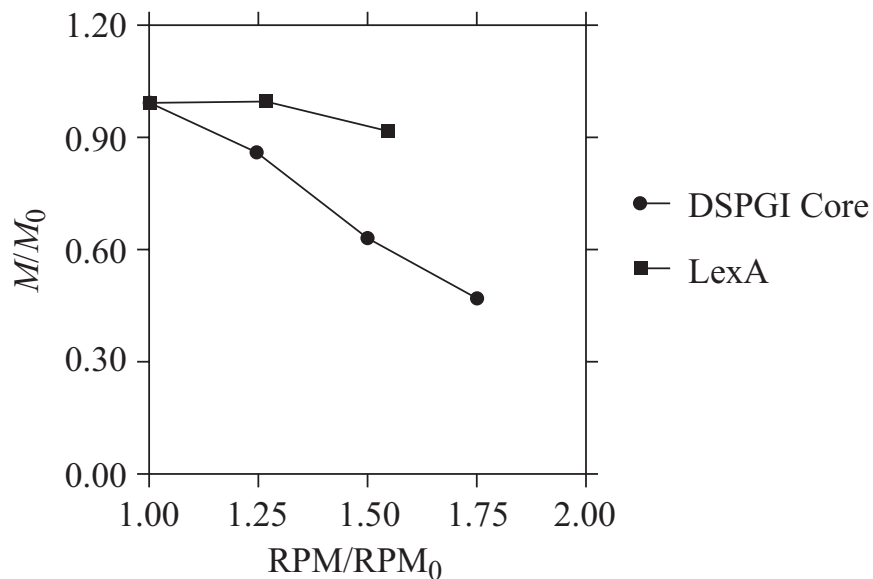


**Figure 3.** Diagnostic graph providing a qualitative characterization of the solution behavior of macromolecules. All data were acquired at a constant temperature between 20 and 25°C. This figure shows the apparent molecular weight (presented as  $M/M_0$ , where  $M_0$  equals the molecular weight determination at the lowest rotor speed) as a function of rotor speed for a homogeneous sample (■) and a heterogeneous sample (●). The x-axis is the ratio of the RPM to the lowest  $RPM_0$  rotor speed used. The homogeneous sample is LexA (0.8 mg/mL) in 50 mM KCl, 20 mM Tris, pH 7.4, 10% sucrose, 2.5 mM  $MgCl_2$ , 1.5 mM  $CaCl_2$ , 0.5 mM EDTA and 1 mM dithiothreitol, and analyzed at rotor speeds of 22,000, 28,000 and 34,000 RPM. LexA ( $M_1 = 23,000$ ) undergoes a reversible monomer-dimer equilibrium such that at this concentration  $M_0 = 35,000$ . The lack of any apparent change in the molecular weight with increasing rotor speed is thermodynamic proof that the equilibrium is fully reversible (3, 12). The heterogeneous sample is core protein from bovine articular cartilage dermatan sulfate proteoglycan I (1.1 mg/mL) in 0.1 M NaCl, 50 mM Tris, pH 7.6, and 5 mM EDTA analyzed at 16,000, 20,000, 24,000 and 28,000 rpm. The pronounced decrease in apparent molecular weight with increased rotor speed in this case is indicative of sample heterogeneity.

A few cautions are in order. First, macromolecular association and thermodynamic nonideality produce opposite effects on the concentration dependence of the molecular weight. Cases have been reported in which what appears to be ideal behavior actually results from compensating effects of association and nonideality. If this is of concern, it can be tested by reexamining the solution under slightly different conditions of pH or salt (11). Second, these graphs are better thought of as qualitative guides and should not be used to estimate association nonideality or molecular weights. For example, mass-action dimer formation will yield an  $M_z$  that is 80% of dimer at the concentration equaling the dissociation constant ( $K_d$ ). Therefore, using the concentration at which  $M_z$  is one-half that of the dimer would yield a serious underestimate of  $K_d$ . These parameters are best determined using the curve fitting methods described above (3, 4). On the other hand, curves like those in Fig. 2 certainly can lead to plausible models for such curve fitting.

### Sample Recovery

One of the attractive features of sedimentation analysis is that it is nondestructive to the sample, and it is possible to recover much of the sample from a short column centerpiece. To do this, the centerpiece is held in place using a fill-hole screw while the top window is removed. To facilitate removing the window, we have drilled two small holes into the top rim of the window holder so that screws may be inserted to serve as handles. (Similar modifications are available from Beckman Coulter on a special request basis.) There is inevitable loss of liquid to the window as it is lifted off, but the majority of it remains in the holes. Once the window is off, the samples may be removed using a micropipette equipped with a microcapillary tip. Typically 70% or so of the initial 14  $\mu$ L is recovered. Procedures for optimizing sample recovery have not been described, so it is possible that even greater quantities could be retrieved.

### Summary

Short column sedimentation equilibrium provides a rapid and sure method for characterizing the solution behavior of macromolecules. The small quantity of material required and the ability to recover the sample unharmed make it an attractive method for molecular biology. Short columns are particularly useful for conducting rapid surveys of the environmental influences on macromolecular association.

## Acknowledgment

The work presented here was supported by a National Science Foundation grant DIR 90-02027. The author thanks Daryl Lyons and Jun Liu for providing the experimental data presented here; Dr. Lawrence Rosenberg for providing articular cartilage link protein, dermatan sulfate proteoglycan core protein and GAG chains; Dr. John Little for providing Lex A; and Dr. Rachel Klevit for providing MyoD-bHLH peptide.

## References

1. van Holde, K. E., Baldwin, R. L. Rapid attainment of sedimentation equilibrium. *J. Phys. Chem.* 62, 734-749 (1958)
2. Yphantis, D. A. Rapid determination of molecular weights of peptides and proteins. *Ann. N. Y. Acad. Sci.* 88, 586-601 (1960)
3. Johnson, M. L., Correia, J. J., Yphantis, D. A., Halvorson, H. R. Analysis of data from the analytical ultracentrifuge by nonlinear least-squares techniques. *Biophys. J.* 36, 575-588 (1981)
4. Correia, J. J., Yphantis, D. A. Equilibrium sedimentation in short columns. *Analytical Ultracentrifugation in Biochemistry and Polymer Science*. Edited by S. Harding and A. Rowe. London, Royal Society for Chemistry, (in press).
5. Christopherson, R. I., Jones, M. E., Finch, L. R. A simple centrifuge column for desalting protein solutions. *Anal. Biochem.* 100, 184-187 (1979)
6. Laue, T. M., Shah, B. D., Ridgeway, T. M., Pelletier, S. L. Computer-aided interpretation of analytical sedimentation data for proteins. *Analytical Ultracentrifugation in Biochemistry and Polymer Science*. Edited by S. Harding and A. Rowe. London, Royal Society for Chemistry, (in press).
7. Durschlag, H. *Thermodynamic Data for Biochemistry and Biotechnology*, Chapter 3, p. 45. Edited by H.-J. Hinz. New York, Springer-Verlag, 1986.
8. Luckow, E. A., Lyons, D. A., Ridgeway, T. M., Esmon, C. T., Laue, T. M. Interaction of clotting factor V heavy chain with prothrombin and prethrombin 1 and role of activated protein C in regulating this interaction: analysis by analytical ultracentrifugation. *Biochemistry* 28, 2348-2354 (1989)
9. Olsen, P. H., Esmon, N. L., Esmon, C. T., Laue, T. M. Ca<sup>2+</sup> dependence of the interactions between protein C, thrombin, and the elastase fragment of thrombomodulin. Analysis by ultracentrifugation. *Biochemistry* 31, 746-754 (1992)
10. Arakawa, T., Yphantis, D. A. Molecular weight of recombinant human tumor necrosis factor- $\alpha$ . *J. Biol. Chem.* 262, 7484-7485 (1987)
11. Wills, P. R. Thermodynamic non-ideality and sedimentation analysis. *Analytical Ultracentrifugation in Biochemistry and Polymer Science*. Edited by S. Harding and A. Rowe. London, Royal Society for Chemistry, (in press).
12. Squire, P. G., Li, C. H. Adrenocorticotropin (ACTH). XXIII. A sedimentation study of the state of aggregation of ovine pituitary ACTH in acidic and basic solutions. *J. Am. Chem. Soc.* 83, 3521-3528 (1961)



Beckman Coulter, the stylized logo, and the Beckman Coulter product and service marks mentioned herein are trademarks or registered trademarks of Beckman Coulter, Inc. in the United States and other countries.

For Beckman Coulter's worldwide office locations and phone numbers, please visit "Contact Us" at [beckmancoulter.com](http://beckmancoulter.com)

CENT-1323APP12.15-A